J|A|C|S
ARTICLES
Published on Web 08/18/2006

Edge-Bridged $Mo_2Fe_6S_8$ to P^N-Type $Mo_2Fe_6S_9$ Cluster Conversion: Structural Fate of the Attacking Sulfide/Selenide Nucleophile

Curtis P. Berlinguette and R. H. Holm*

Contribution from the Department of Chemistry and Chemical Biology, Harvard University, Cambridge, Massachusetts 02138

Received May 23, 2006; E-mail: holm@chemistry.harvard.edu

Abstract: Reaction of the edge-bridged double cubane cluster $[(Tp)_2M_2Fe_6S_8(PEt_3)_4]$ (**1**; Tp = hydrotris(pyrazolyl)borate(1−)) with hydrosulfide affords the clusters $[(Tp)_2M_2Fe_6S_9(SH)_2]^{3-,4-}$ (M = Mo (**2**), V), which have been established as the first structural (topological) analogues of the P^N cluster of nitrogenase. The synthetic reaction is an example of core conversion, resulting in the transformation $M_2Fe_6(\mu_3\text{-}S)_6(\mu_4\text{-}S)_2$ (C_i) → $M_2Fe_6(\mu_2\text{-}S)_2(\mu_3\text{-}S)_6(\mu_6\text{-}S)$ (C_{2v}), the reaction pathway of which is unknown. The most prominent structural feature of P^N-type clusters is the μ_6-S atom, which bridges six iron atoms in two MFe_3S_3 cuboidal halves of the cluster. The initial issue in core conversion is the origin of the μ_6-S atom. Utilizing SeH^- as a surrogate reactant for SH^- in the system **1**/SeH^-/L^- in acetonitrile, a series of selenide clusters $[(Tp)_2Mo_2Fe_6S_8SeL_2]^{3-}$ ($L^- = SH^-$ (**4**), SeH^- (**5**), EtS^- (**6**), CN^- (**7**)) was prepared. The electrospray mass spectra of **4** and **6** revealed inclusion of one Se atom in each cluster, and ^1H NMR spectra and crystallographic refinements of **4**−**7** indicated that this atom was disordered over the two μ_2-S/Se positions. The clusters $\{[(Tp)_2Mo_2Fe_6S_9](\mu_2\text{-}S)\}_2^{5-}$ (**8**) and $\{[(Tp)_2Mo_2Fe_6S_8Se](\mu_2\text{-}Se)\}_2^{5-}$ (**9**) were prepared from **2** and **5**, respectively, and shown to be isostructural. They consist of two P^N-type cluster units bridged by two μ_2-S or μ_2-Se atoms. It is concluded that, in the preparation of **2**, the probable structural fate of the attacking nucleophile is as a μ_2-S atom, and that the μ_3-S and μ_6-S atoms of the product cluster derive from precursor cluster **1**. Cluster fragmentation during P^N-type cluster synthesis is unlikely.

Introduction

In seeking synthetic pathways to meaningful analogues of the P cluster and iron−molybdenum cofactor cluster of nitrogenase,[1−5] we have utilized appropriately ligated edge-bridged double cubane (EBDC) clusters with the heterometal cores $M_2Fe_6S_8$ (M = Mo,[6−8] V[9]) as precursors. This choice is based on the nuclearity and composition of the clusters, which approach those of the P^N ($Fe_8S_7(\mu_2\text{-}S_{Cys})_2$) and iron−molybdenum cofactor ($MoFe_7S_9X$; X = C, N, or O)[4] clusters of the enzyme. A significant transformation based on EBDCs is illustrated in Scheme 1. Here the $M_2Fe_6S_8 = M_2Fe_6(\mu_3\text{-}S)_6(\mu_4\text{-}S)_2$ core is transformed to the $M_2Fe_6S_9 = M_2Fe_6(\mu_2\text{-}S)_2(\mu_3\text{-}S)_6(\mu_6\text{-}S)$ core in a reaction of *core conversion* effected by an attacking sulfide nucleophile. The most conspicuous structural features of the product cluster are the μ_6-S atom and the large exterior Fe−(μ_6-S)−Fe angle (140−147°), features present in the native P^N cluster. Best-fit root-mean-square deviations in atomic positions upon superposition of synthetic and native core units are 0.33−0.36 Å,[10] justifying description of the synthetic clusters as structural (topological) analogues of the P^N state of the enzyme cluster. These clusters are not chemical analogues because of the presence of heterometal atoms and the absence of thiolate bridges. The μ_2-S atoms simulate cysteinate bridging. We describe such species as P^N-type clusters. An all-iron cluster resembling the P^N cluster has been synthesized by a self-assembly procedure.[11] The core conversion reaction has been extensively pursued,[7,8,12−14] with clusters such as $[(Tp)_2M_2Fe_6S_8(PEt_3)_4]$ and $[(Tp)_2Mo_2Fe_6S_8L_4]^{4-,3-}$ (L = halide, Tp = hydrotris(pyrazolyl)borate(1−)) serving as starting materials.

Core conversion is one of several synthetic methodologies directed toward the attainment of weak-field clusters.[10] A conversion comparable to that shown in Scheme 1 had not been encountered prior to or since our initial observation.[12] Because of its uniqueness and salience in reaching clusters related to those in nitrogenase, the pathway of core conversion is a matter

(1) Peters, J. W.; Stowell, M. H. B.; Soltis, S. M.; Finnegan, M. G.; Johnson, M. K.; Rees, D. C. *Biochemistry* **1997**, *36*, 1181−1187.
(2) Smith, B. E. *Adv. Inorg. Chem.* **1999**, *47*, 160−218.
(3) Mayer, S. M.; Lawson, D. M.; Gormal, C. A.; Roe, S. M.; Smith, B. E. *J. Mol. Biol.* **1999**, *292*, 871−891.
(4) Einsle, O.; Tezcan, F. A.; Andrade, S. L. A.; Schmid, B.; Yoshida, M.; Howard, J. B.; Rees, D. C. *Science* **2002**, *297*, 1696−1700.
(5) Rees, D. C.; Tezcan, F. A.; Haynes, C. A.; Walton, M. Y.; Andrade, S.; Einsle, O.; Howard, J. B. *Philos. Trans. R. Soc. A* **2005**, *363*, 971−984.
(6) Fomitchev, D. V.; McLauchlan, C. C.; Holm, R. H. *Inorg. Chem.* **2002**, *41*, 958−966.
(7) Zhang, Y.; Holm, R. H. *J. Am. Chem. Soc.* **2003**, *125*, 3910−3920.
(8) Berlinguette, C. P.; Miyaji, T.; Zhang, Y.; Holm, R. H. *Inorg. Chem.* **2006**, *45*, 1997−2007.
(9) Hauser, C.; Bill, E.; Holm, R. H. *Inorg. Chem.* **2002**, *41*, 1615−1624.
(10) Lee, S. C.; Holm, R. H. *Chem. Rev.* **2004**, *104*, 1135−1157.
(11) Ohki, Y.; Sunada, Y.; Honda, M.; Katsada, M.; Tatsumi, K. *J. Am. Chem. Soc.* **2003**, *125*, 4052−4053.
(12) Zhang, Y.; Zuo, J.-L.; Zhou, H.-C.; Holm, R. H. *J. Am. Chem. Soc.* **2002**, *124*, 14292−14293.
(13) Zuo, J.-L.; Zhou, H.-C.; Holm, R. H. *Inorg. Chem.* **2003**, 4624−4631.
(14) Zhang, Y.; Holm, R. H. *Inorg. Chem.* **2004**, *43*, 674−682.

Scheme 1. Conversion of Edge-Bridged Double Cubane Clusters to P^N-Type Clusters with M = Mo[6–8] and V[9] in Previous Work; Terminal Ligands and Cluster Oxidation States Are Indicated

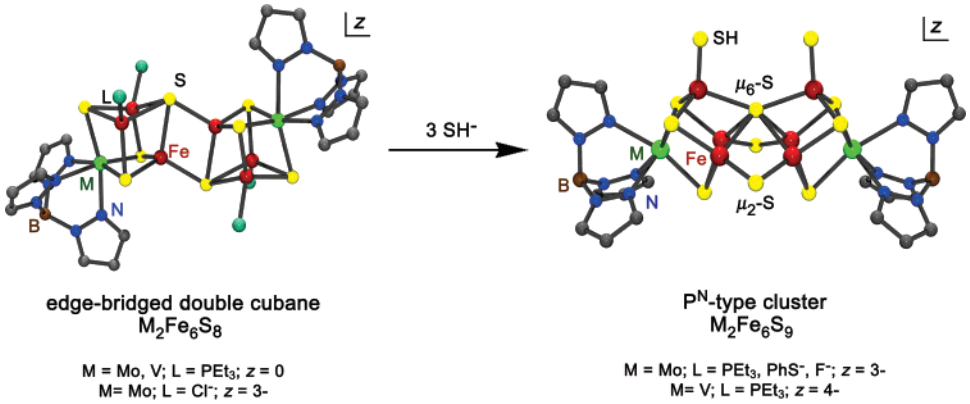

Table 1. Crystallographic Data for Compounds Containing the Clusters $[(Tp)_2Mo_2Fe_6S_8Se(SH)_2]^{3-}$ (**4**), $[(Tp)_2Mo_2Fe_6S_8Se(SeH)_2]^{3-}$ (**5**), $[(Tp)_2Mo_2Fe_6S_8Se(SEt)_2]^{3-}$ (**6**), $[(Tp)_2Mo_2Fe_6S_8Se(CN)_2]^{3-}$ (**7**), and $\{[(Tp)_2Mo_2Fe_6S_9](\mu_2\text{-}S)\}_2^{5-}$ (**8**)[a]

	$(Et_4N)_3$[**4**]·2.75 MeCN	$(Et_4N)_3$[**5**]·5.5MeCN	$(Et_4N)_3$[**6**]·MeCN	$(Et_4N)_3$[**7**]·2.5MeCN	$(Et_4N)_5$[**8**]·8MeCN
formula	$C_{47.5}H_{90.25}B_2Fe_6Mo_2N_{17.75}S_{10.08}Se_{0.92}$	$C_{53}H_{98.5}B_2Fe_6Mo_2N_{20.5}S_{7.96}Se_{3.04}$	$C_{48}H_{93}B_2Fe_6Mo_2N_{16}S_{9.91}Se_{1.09}$	$C_{49}H_{87.5}B_2Fe_6Mo_2N_{19.5}S_{7.8}Se_{1.2}$	$C_{92}H_{164}B_4Fe_{12}Mo_4N_{37}S_{20}$
fw	1854.5	2066.8	1846.8	1843.3	3502.8
cryst system	monoclinic	monoclinic	triclinic	monoclinic	orthorhombic
space group	$P2_1/m$	$P2_1/m$	$P\bar{1}$	$P2_1/m$	$Aba2$
Z	2	2	2	2	4
a, Å	16.048(2)	16.18(3)	14.98(5)	16.607(2)	36.478(9)
b, Å	17.736(3)	17.74(2)	17.10(6)	17.385(2)	26.208(7)
c, Å	18.142(3)	18.24(2)	18.49(7)	18.396(3)	16.165(6)
α, deg	90	90	91.50(2)	90	90
β, deg	115.46(1)	116.2(1)	101.83(2)	116.816(2)	90
γ, deg	90	90	115.15(9)	90	90
V, Å^3	4660(10)	4700(10)	4160(3)	4740(1)	15454(8)
GOF (F^2)	1.142	1.052	1.044	1.051	1.147
R_1,[b] wR_2[c]	0.086, 0.25	0.056, 0.17	0.081, 0.22	0.063, 0.18	0.088, 0.19
S/Se ratio[d]	0.54/0.46	0.48/0.52	0.48/0.52; 0.43/0.57	0.40/0.60	n/a

[a] Collected using Mo Kα radiation (λ = 0.71073 Å) at T = 213 K. [b] $R(F_o) = \sum[(F_o - F_o)]/\sum(F_o)$. [c] $R_w(F_o^2) = \{\sum[w(F_o^2 - F_c^2)^2/\sum[w(F_o^2)^2]\}^{1/2}$. [d] μ_2-S/Se site.

of interest. While in our experience the reactant and product clusters appear to be stable under strictly anaerobic, nonprotic ambient conditions, a potential complication in arriving at a pathway description is the formation of cluster fragments under the influence of nucleophilic attack. Thereafter, the fragments combine to afford the product structure. Examination of this possible situation requires the inclusion in the reaction system of isotopic or radioactive tracer components subject to incorporation in the product should cluster fracture occur. Such experiments would be expensive, and their design is nontrivial. In the absence of a cluster fragment scenario, the recurring complexity of the reaction can be appreciated by the realization that 18 Fe−S bonds are expanded to 22 such bonds in the P^N-type product in the structures as written. Some six M−S bonds are apparently preserved; indeed, Mo−S bonds are expected to be substantially less labile than Fe−S interactions. We take as the initial issue to be addressed in core conversion the origin of the μ_6-S atom in the product cluster. Does it derive from the reactant cluster or the attacking sulfide? The present work provides a more detailed investigation of this matter than reported heretofore.[7]

Experimental Section

Preparation of Compounds. All reactions and manipulations were performed under a pure dinitrogen atmosphere using either Schlenk techniques or an inert atmosphere box. Solvents were passed through an Innovative Technology solvent purification system prior to use. The compounds $[(Tp)_2Mo_2Fe_6S_8(PEt_3)_4]$, $(Et_4N)_3[(Tp)_2Mo_2Fe_6S_9(SH)_2]$ (ESMS: m/z 654.1 (calcd for $\{M\}^{2-}$ 654.2), 1438.0 (calcd for $\{M^{2-} + Et_4N^+\}^-$ 1437.6)), and $(Et_4N)_5\{[(Tp)_2Mo_2Fe_6S_8Se](\mu_2\text{-}Se)\}_2$ (see below) were prepared as described.[7] The compound $(Et_4N)(SeH)$ was prepared by the method described for the Me_4N^+ salt.[15] The five compounds in Table 1 were characterized by X-ray structure determinations. Because of the small scale of the preparations, isolated compounds were not analyzed. However, like EBDCs,[8] P^N-type clusters display distinctive isotropically shifted ^{1}H NMR spectra, fully consistent with solid-state structures and satisfactory purity of isolated compounds. For most cluster salts, parent ions with isotope distributions consistent with the formulations given were observed in electrospray mass spectra.

$(Et_4N)_3[(Tp)_2Mo_2Fe_6S_9(CN)_2]$. To a suspension of 50 mg (0.030 mmol) of $[(Tp)_2Mo_2Fe_6S_8(PEt_3)_4]$ in 3 mL of acetonitrile was added 15 mg (0.092 mmol) of $(Et_4N)(SH)$ in 2 mL of acetonitrile. The reaction mixture was stirred for 1 h, 10 mg (0.064 mmol) of $(Et_4N)(CN)$ was added, and stirring was continued for 1 h. The solution was filtered through Celite. Vapor diffusion of ether into the red-black filtrate maintained at −35 °C afforded the product as 30 mg (58%) of black block-like crystals. ^{1}H NMR (CD_3CN, anion): δ 5.32 (2), 7.21 (br, B−H), 9.28 (1), 11.2 (br, 2), 14.08 (1), 17.9 (vbr, 1), 18.92 (2).

$(Et_4N)_3[(Tp)_2Mo_2Fe_6S_8Se(SH)_2]$. To a suspension of 51 mg (0.030 mmol) of $[(Tp)_2Mo_2Fe_6S_8(PEt_3)_4]$ in 5 mL of acetonitrile was added 19 mg (0.090 mmol) of $(Et_4N)(SeH)$ in 1 mL of acetonitrile. The

(15) Batchelor, R. J.; Einstein, F. W. B.; Gay, I. D.; Jones, C. H. W.; Sharma, R. D. *Inorg. Chem.* **1993**, *32*, 4378−4383.

reaction mixture was stirred for 1 h and filtered through Celite. A solution of 10 mg (0.061 mmol) of $(Et_4N)(SH)$ in 2 mL of acetonitrile was added to the filtrate. The solution was stirred for 1 h and filtered through Celite. Vapor diffusion of ether into the black filtrate at −35 °C gave the product as 44 mg (84%) of black platelets. ESMS: *m*/*z* 1746.0 (calcd for $\{M^{2-} + 3Et_4N^+\}^+$ 1745.8). ^{1}H NMR (CD_3CN, anion): δ 5.06 (1), 5.40 (1), 5.7 (br, B−H), 8.06 (1), 11.4 (br, 1), 13.4 (br, 1), 13.46 (1), 16.33 (1), 16.45 (1), 20.2 (vbr, 1).

$(Et_4N)_3[(Tp)_2Mo_2Fe_6S_8Se(SeH)_2]$. To a suspension of 56 mg (0.033 mmol) of $[(Tp)_2Mo_2Fe_6S_8(PEt_3)_4]$ in 5 mL of acetonitrile-d_3 was added 23 mg (0.11 mmol) of $(Et_4N)(SeH)$ in 3 mL of acetonitrile. The dark green mixture was stirred for 1 h and filtered through Celite to afford a green-black filtrate. ^{1}H NMR (CD_3CN, anion): δ 5.07 (1), 5.34 (1), 5.9 (br, B−H), 8.45 (1), 11.4 (br, 1), 13.3 (br, 1), 13.58 (1), 16.63 (1), 16.75 (1), 21.9 (vbr, 1). No other cluster signals were observed in the filtrate, indicating an essentially quantitative conversion to product. Vapor diffusion of ether into the filtrate at −35 °C led to isolation of the compound as 56 mg (92%) of black platelets.

$(Et_4N)_3[(Tp)_2Mo_2Fe_6S_8Se(SEt)_2]$. To a suspension of 51 mg (0.030 mmol) of $[(Tp)_2Mo_2Fe_6S_8(PEt_3)_4]$ in 5 mL of acetonitrile was added 19 mg (0.090 mmol) of $(Et_4N)(SeH)$ in 3 mL of acetonitrile. The reaction mixture was stirred for 1 h. A solution of 12 mg (0.063 mmol) of $(Et_4N)(SEt)$ in 3 mL of acetonitrile was added. The mixture was stirred for 1 h and filtered through Celite. Vapor diffusion of ether into the deep green filtrate led to separation of the product as 43 mg (79%) of black needle-like crystals. ESMS: *m*/*z* 706.0 (calcd for $\{M\}^{2-}$ 706.2), 1541.9 (calcd for $\{M^{2-} + Et_4N^+\}^-$ 1541.6). ^{1}H NMR (CD_3CN, anion): δ 4.01 (SCH_2CH_3), 5.04 (1), 5.26 (1), 5.3 (br, B−H), 7.06 (1), 11.2 (br, 1), 12.58 (1), 13.1 (br, 1), 15.91 (1), 16.04 (1), 16.8 (vbr, 1). The SCH_2 signal was not located, probably because of paramagnetic broadening.

$(Et_4N)_3[(Tp)_2Mo_2Fe_6S_8Se(CN)_2]$. To a suspension of 53 mg (0.031 mmol) of $[(Tp)_2Mo_2Fe_6S_8(PEt_3)_4]$ in 5 mL of acetonitrile was added 20 mg (0.095 mmol) of $(Et_4N)(HSe)$ in 3 mL of acetonitrile. The reaction mixture was stirred for 1 h. A solution of 10 mg (0.065 mmol) of $(Et_4N)(CN)$ in 3 mL of acetonitrile was added. The mixture was stirred for 20 min and filtered through Celite. Vapor diffusion of ether into the deep red filtrate afforded the product as 21 mg (38%) of black platelets. ^{1}H NMR (CD_3CN, anion): δ 5.27 (1), 5.50 (1), 7.10 (br, B−H), 9.09 (1), 10.9 (br, 1), 12.3 (br, 1), 14.17 (1), 17.7 (vbr, 1), 18.69 (1), 18.84 (1).

$(Et_4N)_5\{[(Tp)_2Mo_2Fe_6S_9](\mu_2\text{-}S)\}_2$. A solution containing 84 mg (0.049 mmol) of $(Et_4N)_3[(Tp)_2Mo_2Fe_6S_9(SH)_2]$ in 8 mL of acetonitrile was stirred for 4 h at 65 °C. The solution was cooled and filtered through Celite. Vapor diffusion of ether into the black filtrate led to separation of the product as 12 mg (15%) of black needle-like crystals. The low yield is attributed to decomposition of the initial cluster during heating to form $(Et_4N)_2[(Tp)MoFe_3S_4(SH)_3]$,[7] which was detected in the ^{1}H NMR spectrum of the product.

$(Et_4N)_5\{[(Tp)_2Mo_2Fe_6S_8Se](\mu_2\text{-}Se)\}_2$. This procedure leads to a cluster product with the S/Se atom ratio the same as or similar to that reported earlier.[7] To 32 mg (0.017 mmol) of $(Et_4N)_3[(Tp)_2Mo_2Fe_6S_8Se(SeH)_2]$ was added 5 mL of acetonitrile. The mixture was stirred for 4 h and filtered through Celite. Vapor diffusion of ether into the black filtrate yielded the product as 27 mg (93%) of black needle-like crystals. ESMS: *m*/*z* 1969.4 (calcd for $\{[(Tp)_2Mo_2Fe_6S_8Se_3H_2]^{3-} + 4Et_4N^+\}^+$ 1969.9; the parent ion was not observed. The product was identified by correspondence of unit cell parameters with those reported previously.[7]

In the sections that follow, clusters are designated as **1**−**9** according to Chart 1.

Chart 1. Designation of Clusters

$[(Tp)_2Mo_2Fe_6S_8(PEt_3)_4]$	**1**[7]
$[(Tp)_2Mo_2Fe_6S_9(SH)_2]^{3-}$	**2**[7]
$[(Tp)_2Mo_2Fe_6S_9(CN)_2]^{3-}$	**3**
$[(Tp)_2Mo_2Fe_6S_8Se(SH)_2]^{3-}$	**4**
$[(Tp)_2Mo_2Fe_6S_8Se(SeH)_2]^{3-}$	**5**
$[(Tp)_2Mo_2Fe_6S_8Se(SEt)_2]^{3-}$	**6**
$[(Tp)_2Mo_2Fe_6S_8Se(CN)_2]^{3-}$	**7**
$\{[(Tp)_2Mo_2Fe_6S_9](\mu_2\text{-}S)\}_2^{5-}$	**8**
$\{[(Tp)_2Mo_2Fe_6S_8Se](\mu_2\text{-}Se)\}_2^{5-}$	**9**

X-ray Structure Determinations. The structures of the five compounds in Table 1 were determined. Suitable crystals of solvated forms of $(Et_4N)_3$[**6**,**7**] and $(Et_4N)_5$[**8**] were obtained by ether diffusion into acetonitrile solutions at 273 K for at least 24 h; solvated crystals of $(Et_4N)_3$[**3**,**4**,**5**] were acquired by ether diffusion into an acetonitrile solution at 238 K for at least 72 h. Crystals were coated with paratone-N oil and mounted on a Bruker APEX CCD-based diffractometer equipped with an LT-2 low-temperature apparatus operating at 213 K. Data were collected with scans of 0.3 s/frame for 30 s, so that 1271−1850 frames were collected for a hemisphere of data. The first 50 frames were recollected at the end of the data collection to monitor for decay; no significant decay was detected for any compound. Cell parameters were retrieved with SMART software and refined using SAINT software on all reflections. Data integration was performed with SAINT, which corrects for Lorenz polarization and decay. Absorption corrections were applied using SADABS. Space groups were assigned unambiguously by analysis of symmetry and systematic absences determined by XPREP. The compound $(Et_4N)_3$[**7**]·2.5MeCN occurred as a twinned crystal, as determined by the TwinRotMax routine in PLATON and confirmed by ROTAX software. The data were detwinned by incorporation of TWIN instruction in SHELXTL with the matrix −1 0 0, 0 −1 0, 1 0 1. Missing symmetry in all crystals was checked with PLATON; none was found.

In the foregoing compounds, clusters **3**−**5** and **7** contain a mirror plane passing through the two Mo atoms and the μ_6-S atom. The asymmetric unit for each of these compounds consists of one-half anion, one cation refined to full occupancy, one cation refined to half-occupancy, and a variable number of acetonitrile solvate molecules. The Tp ligand bound to Mo2 in **3**−**5** and **7** deviates from the plane of symmetry; the resulting disorder was modeled accordingly. In **8**, one-half of the cluster comprises the asymmetric unit, and the two P^N-type cluster units and μ_2-Se atoms bridging these units are related by a C_2 axis. The asymmetric unit of **6** contains the entire cluster.

For compounds containing clusters **4**−**7**, the relative occupancy of S and Se atoms at the μ_2-S/Se sites was established by expressing the occupation factors in terms of a free variable so that the sum was constrained to a constant value of 1.0. The *xyz* and U_{ij} parameters were equated for the S/Se atoms sharing the same site. This procedure was also used to establish that the μ_2-Se sites spanning individual P^N-like clusters in **8** are exclusively populated by Se atoms, and that there was no significant population of Se atoms at μ_3- and μ_6-sites in any cluster. Structures were solved by direct methods and refined against all data by full-matrix least-squares techniques on F^2 using the SHELXTL-97 package. All non-hydrogen atoms were refined anisotropically. Hydrogen atoms were placed at idealized positions on carbon atoms. Crystal parameters and agreement factors are reported in Table 1.[16]

The compound $(Et_4N)_3$[**3**]·∼7MeCN crystallizes in monoclinic space group $P2_1/m$ with a =16.630(7) Å, b = 17.199(6) Å, c = 18.275(5) Å, β = 116.25(3)°, V = 4690(10) Å^3, and Z = 2. Data refinement verified the identity of the cluster, certain metric features, and the presence of three counterions. However, disorder of the Tp ligand, one cation, and solvate molecules prevented a satisfactory refinement (R_1 = 0.13, wR_2 = 0.34).

Other Physical Measurements. All measurements were performed under anaerobic conditions. ^{1}H NMR spectra were obtained with a

(16) See paragraph at the end of this article for a summary of the Supporting Information available.

Scheme 2. Reaction Scheme Depicting Conversion of Edge-Bridged Double Cubane Cluster **1** to P^N-Type Clusters **2** and **5**, Their Conversion to Other P^N-type Clusters **3**, **4**, **6**, and **7** by Ligand Substitution, and the Formation of Bridged Double P^N-Type Clusters **8** and **9**

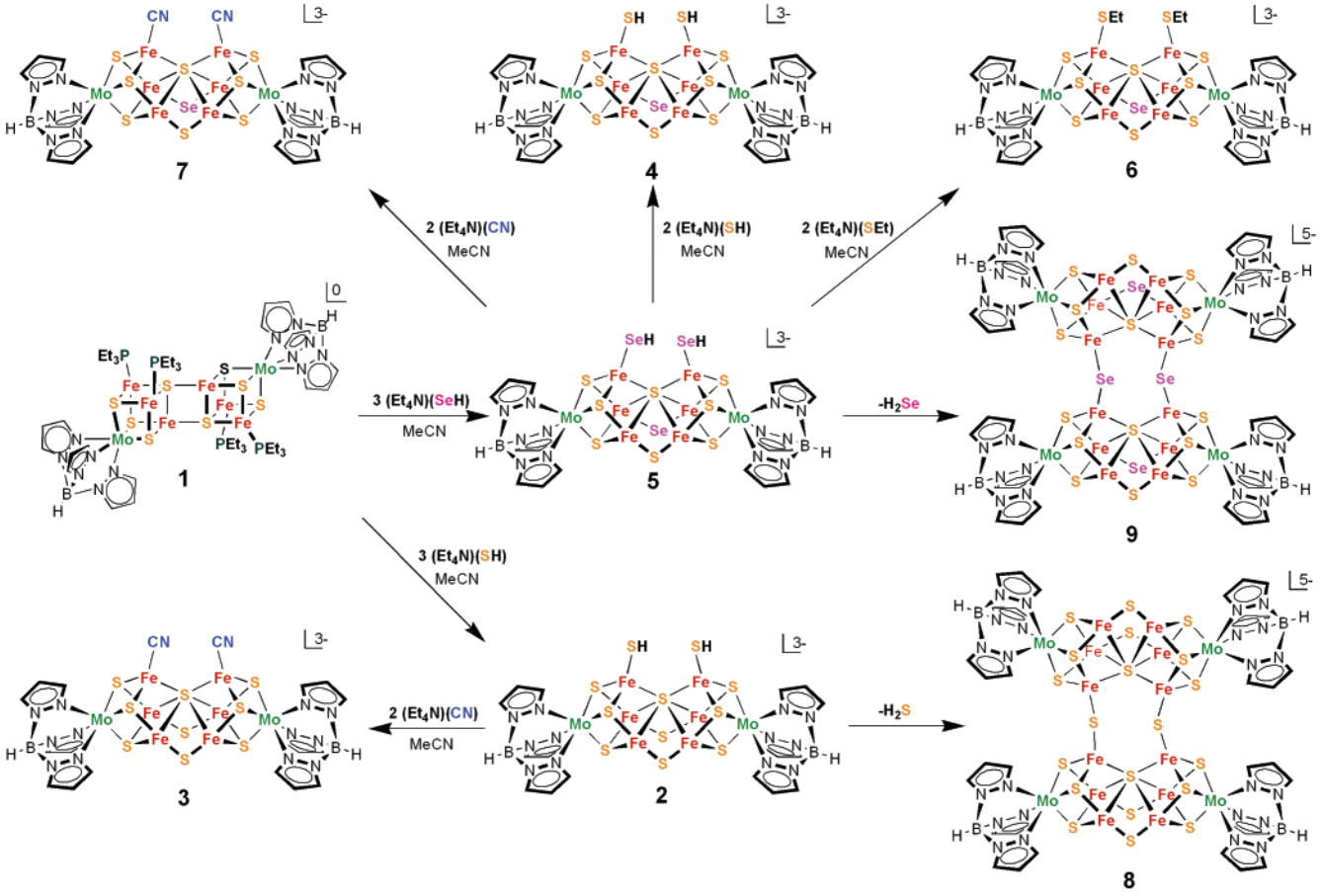

Varian AM-400 spectrometer. Electrochemical measurements were made with a Princeton Applied Research model 263 potentiostat/galvanostat using acetonitrile solutions, a glassy carbon working electrode, and 0.1 M (Bu_4N)(PF_6) supporting electrolyte. Potentials are referenced to a standard calomel electrode (SCE). Electrospray mass spectra were recorded on acetonitrile solutions (10 mM) directly infused into an LCT mass spectrometer at a flow rate of 5 μL/min. Compounds containing **2** and **6** were recorded in the negative mode with the capillary voltage held constant at −3700 kV, the cone voltage set at +50 V, and the extraction cone voltage set at +4 V. The desolvation and source temperatures were 300 and 120 °C, respectively. Compounds containing **4**, **5**, and **9** were observed only in the positive mode with the capillary, cone, and extraction cone voltages set at +3700, −50, and −5 V, respectively.

Results and Discussion

The matter at issue is the nature of the core conversion $M_2Fe_6S_8$ (C_i) → $M_2Fe_6S_9$ (C_{2v}) depicted in Scheme 1. While a similar structural alteration can be effected with other nucleophiles, such as ethanethiolate and methoxide,[14] the reaction with hydrosulfide is of prime interest because of the composition of the product cluster. Reactions pertinent to this investigation are set out in Scheme 2. These originate with phosphine-ligated EBDC **1**, which upon direct reaction with nucleophiles QH^- (Q = S, Se) is converted to P^N-type clusters **2** and **5**. These clusters undergo terminal ligand substitution with retention of structure to afford **3**−**7**, and terminal ligand elimination to produce the bridged clusters **8** and **9**. Clusters were identified by isotropically shifted ^{1}H NMR spectra, X-ray structure determinations, and/or electrospray mass spectra (three clusters). The structures of all clusters are depicted in Scheme 2.

To investigate the locus of the attacking nucleophile in the product core, we have utilized hydroselenide as a surrogate reactant for hydrosulfide. Sets of weak-field sulfide/selenide clusters with corresponding compositions and the same or very similar terminal ligands are known and include those with rhomboidal Fe_2Q_2,[17,18] cuboidal and linear Fe_3Q_4,[18,19] cubane-type Fe_4Q_4,[20−24] Fe_6Q_9,[19,25,26] and heterometal cubane-type MFe_3S_4 (M = Mo,[27,28] Ni[29]) cores. In these clusters, selenide substitution of sulfide conserves structures and induces several

(17) Mayerle, J. J.; Denmark, S. E.; DePamphilis, B. V.; Ibers, J. A.; Holm, R. H. *J. Am. Chem. Soc.* **1975**, *97*, 1032−1045. The structure of $[Fe_4S_4(S\text{-}p\text{-}C_6H_4Me)_4]^{2-}$ was determined at room temperature.
(18) Yu, S.-B.; Papaefthymiou, G. C.; Holm, R. H. *Inorg. Chem.* **1991**, *30*, 3476−3485. The structure of $[Fe_4Se_4(SPh)_4]^{2-}$ was determined at −170 K.
(19) Hagen, K. S.; Watson, A. D.; Holm, R. H. *J. Am. Chem. Soc.* **1983**, *105*, 3905−3913.
(20) Que, L., Jr.; Bobrik, M. A.; Ibers, J. A.; Holm, R. H. *J. Am. Chem. Soc.* **1974**, *96*, 4168−4178.
(21) Bobrik, M. A.; Laskowski, E. J.; Johnson, R. W.; Gillum, W. O.; Berg, J. M.; Hodgson, K. O.; Holm, R. H. *Inorg. Chem.* **1978**, *17*, 1402−1410.
(22) Carney, M. J.; Papaefthymiou, G. C.; Whitener, M. A.; Spartalian, K.; Frankel, R. B.; Holm, R. H. *Inorg. Chem.* **1988**, *27*, 346−352.
(23) Stack, T. D. P.; Holm, R. H. *J. Am. Chem. Soc.* **1988**, *110*, 2484−2494.
(24) Stack, T. D. P.; Weigel, J. A.; Holm, R. H. *Inorg. Chem.* **1990**, *29*, 3745−3760.
(25) Strasdeit, H.; Krebs, B.; Henkel, G. *Inorg. Chem.* **1984**, *23*, 1816−1825.
(26) Strasdeit, H.; Krebs, B.; Henkel, G. *Z. Naturforsch.* **1987**, *42b*, 565−572.
(27) Wolff, T. E.; Berg, J. M.; Hodgson, K. O.; Frankel, R. B.; Holm, R. H. *J. Am. Chem. Soc.* **1979**, *101*, 4140−4150.
(28) Greaney, M. A.; Coyle, C. L.; Pilato, R. S.; Stiefel, E. I. *Inorg. Chim. Acta* **1991**, *189*, 81−96.
(29) Ciurli, S.; Ross, P. K.; Scott, M. J.; Yu, S.-B.; Holm, R. H. *J. Am. Chem. Soc.* **1992**, *114*, 5415−5423.

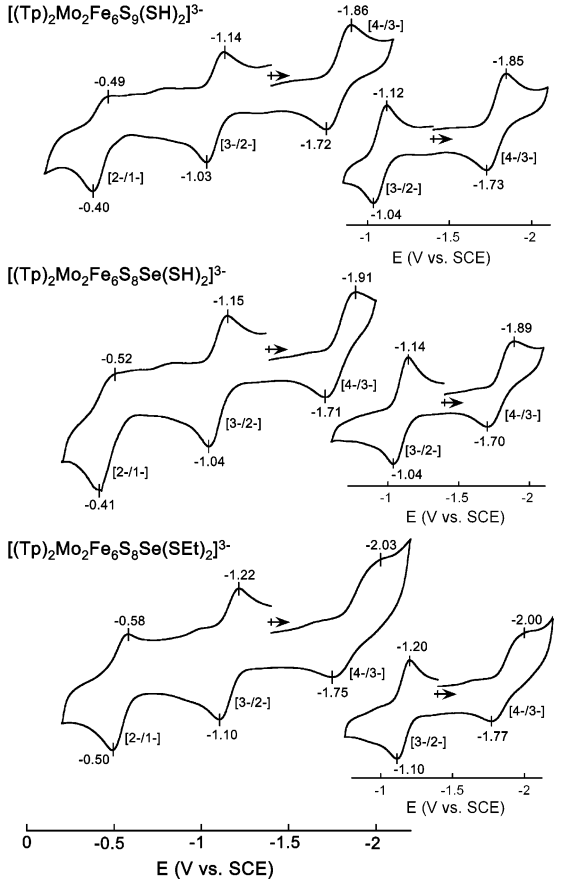

Figure 1. Cyclic voltammograms (100 mV/s) of $[(Tp)_2Mo_2Fe_6S_9(SH)_2]^{3-}$ (**2**), $[(Tp)_2Mo_2Fe_6S_8Se(SH)_2]^{3-}$ (**4**), and $[(Tp)_2Mo_2Fe_6S_8Se(SEt)_2]^{3-}$ (**6**) in acetonitrile at 298 K. Peak potentials for the redox couples [4−/3−], [3−/2−], and [2−/1−] are indicated. The insets emphasize two chemically reversible couples. Certain impurity signals are evident between the main features.

property differences, among them red-shifted LMCT transitions, small positive displacements of redox potentials, and increases in Fe−(μ_{2-4}-Q) bond distances. The last effect encompasses the range 0.10−0.14 Å, with the majority of comparisons at 0.12−0.13 Å. All Fe−(μ_6-S) interactions in synthetic molecular species are found in P^N-type clusters. No discrete species containing an Fe−(μ_6-Se) interaction has been reported.

Prototypic P^N-Type Cluster. The original synthesis of this heterometal cluster type was described by reaction 1,[7] with the one-half equivalent of dihydrogen invoked because the product core ($[Mo_2Fe_6S_9]^+$) is one electron more oxidized than the all-ferrous reactant core. The voltammogram in Figure 1 reveals

$$[(Tp)_2Mo_2Fe_6S_8(PEt_3)_4] + 3SH^- \rightarrow [(Tp)_2Mo_2Fe_6S_9(SH)_2]^{3-} + 4PEt_3 + {}^1/_2H_2 \quad (1)$$

three redox steps for **2**, with the [4−/3−] couple at $E_{1/2} = -1.80$ V not having been detected previously.[7] Consequently, the putative fully reduced cluster $[(Tp)_2Mo_2Fe_6S_9(SH)_2]^{4-}$ is an extremely strong reductant and could be oxidized by a protic source or by trace dioxygen. Redox potentials for this and other P^N-type clusters are collected in Table 2. The ^{1}H NMR spectrum of **2** in Figure 2, containing two sets of pyrazolyl proton resonances in a 2:1 intensity ratio, is consistent with C_{2v} symmetry closely approached in the crystalline state.[7] For **2** and other clusters, certain bond distances are provided in Table 3

Table 2. Redox Potentials for P^N-Type Clusters in Acetonitrile Solution

	$E_{1/2}$ (V)[a]		
cluster	2−/1−	2−/3−	3−/4−
$[(Tp)_2Mo_2Fe_6S_9(SH)_2]^{3-}$ (**2**)	−0.45	−1.09	−1.80
$[(Tp)_2Mo_2Fe_6S_9(CN)_2]^{3-}$ (**3**)	−0.18[b]	−0.94	−1.65
$[(Tp)_2Mo_2Fe_6S_8Se(SH)_2]^{3-}$ (**4**)	−0.47	−1.10	−1.81
$[(Tp)_2Mo_2Fe_6S_8Se(SeH)_2]^{3-}$ (**5**)[c]	−[d]	−1.00	−1.69
$[(Tp)_2Mo_2Fe_6S_8Se(SEt)_2]^{3-}$ (**6**)	−0.54	−1.16	−1.89
$[(Tp)_2Mo_2Fe_6S_8Se(CN)_2]^{3-}$ (**7**)	−0.15[b]	−0.87	−1.58

[a] Vs SCE at 298 K. [b] Irreversible; $E_{p,a}$. [c] Generated *in situ* in the reaction system **1**/(Et_4N)(SeH). [d] Masked by (Et_4N)(HSe).

and selected angular parameters in Table 4. These parameters are related to bridging interactions, which are the structural features of principal interest; complete tabulations of metric parameters are available elsewhere.[16] Because of the detailed structural description of **2** given elsewhere,[7] no such descriptions are required here for **2**−**7**, which are essentially isostructural.

Cluster **2** supports ligand substitution reaction 2 to yield **3**, the X-ray structure of which (not shown) contains as a prominent feature a large external Fe−(μ_6-S)−Fe angle (141.0(1)°), characteristic of all clusters of this type (Table 4). The ^{1}H NMR

$$[(Tp)_2Mo_2Fe_6S_9(SH)_2]^{3-} + 2CN^- \rightarrow [(Tp)_2Mo_2Fe_6S_9(CN)_2]^{3-} + 2SH^- \quad (2)$$

spectrum, shown in Figure 3, corresponds to C_{2v} symmetry. Cyanide coordination causes substantial positive shifts in redox potentials, but a potential of $\lesssim -1.7$ V is still required to generate the fully reduced cluster. Cyanide substitution of $[Fe_4S_4]$ clusters affords a similar positive influence on the redox potentials.[30] Clusters **2** and **3** are valuable as spectroscopic and structural comparisons with selenium-containing clusters.

Selenium-Containing P^N-Type Clusters. Reaction 3, with hydroselenide leading to cluster **5**, is described analogously to reaction 1. In a variation of this reaction system, two equivalents of a ligand are added after reaction with hydroselenide, resulting in formation of the clusters **4**, **6**, and **7** in substitution reaction 4 ($L^- = SH^-$, EtS^-, CN^-).

$$[(Tp)_2Mo_2Fe_6S_8(PEt_3)_4] + 3SeH^- \rightarrow [(Tp)_2Mo_2Fe_6S_8Se(SeH)_2]^{3-} + 4PEt_3 + {}^1/_2H_2 \quad (3)$$

$$[(Tp)_2Mo_2Fe_6S_8Se(SeH)_2]^{3-} + 2L^- \rightarrow [(Tp)_2Mo_2Fe_6S_8SeL_2]^{3-} + 2SeH^- \quad (4)$$

The [4−/3−] redox potentials of all other selenium-containing clusters ($\lesssim -1.7$ V, Table 2) rationalize their isolation in the one-electron oxidized state ($[Mo_2Fe_6S_8Se]^+$). All clusters exhibit the chemically reversible couples [4−/3−] and [3−/2−] ($i_{pa}/i_{pc} \approx 1$) in the −0.9 to −1.9 V interval, consistent with a common core structure.

Comparison of the ^{1}H NMR spectra of **2** and product cluster **5** reveals three inequivalent pyrazolyl rings in a 1:1:1 ratio in the latter (Figure 2). A similar comparison is found between the spectra of cyanide-ligated clusters **3** and **7**; the spectra of **4** and **6** are also indicative of mirror symmetry (Figure 3). The

(30) Scott, T. A.; Berlinguette, C. P.; Holm, R. H.; Zhou, H.-C. *Proc. Natl. Acad. Sci. U.S.A.* **2005**, *102*, 9741−9744.

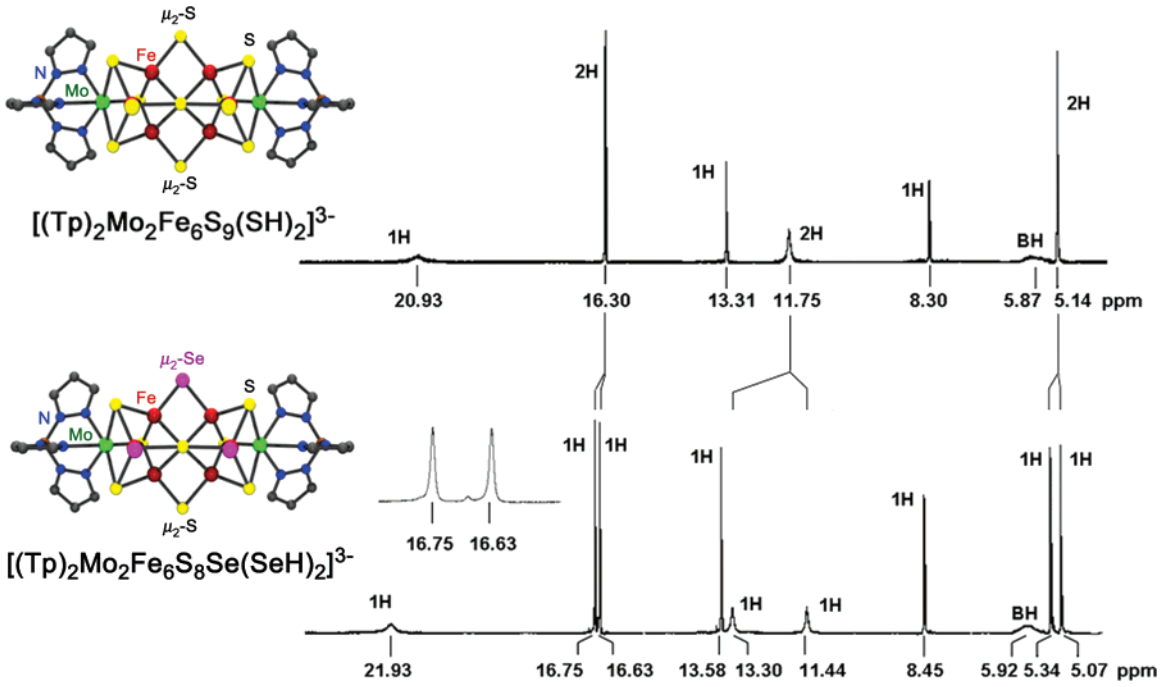

Figure 2. ^{1}H NMR spectra of $[(Tp)_2Mo_2Fe_6S_9(SH)_2]^{3-}$ (**2**, upper) and $[(Tp)_2Mo_2Fe_6S_8Se(SeH)_2]^{3-}$ (**5**, lower) in CD_3CN solutions at ambient temperature. Relative signal intensities are indicated. The 2:1 ratio of equivalent pyrazolyl rings in **2** and the lack of ring equivalence in **9** are illustrated. The inset highlights the two signals centered at ~16.7 ppm in the spectrum of **5**.

Table 3. Selected Mean Values of Bond Distances (Å) in P^N-Type Clusters[a]

cluster	intra[b] Fe–(μ_2-S/Se)	Fe–(μ_6-S)	inter[c] Fe–(μ_2-S/Se)	Fe–L[d]
$[(Tp)_2Mo_2Fe_6S_9(SH)_2]^{3-}$ (**2**)[e]	2.225(5)	2.38(2)		2.29(1)
$[(Tp)_2Mo_2Fe_6S_9(CN)_2]^{3-}$ (**3**)	2.218(6)	2.36(3)		2.04(4)
$[(Tp)_2Mo_2Fe_6S_8Se(SH)_2]^{3-}$ (**4**)	2.302(1)	2.38(1)		2.30(3)
$[(Tp)_2Mo_2Fe_6S_8Se(SeH)_2]^{3-}$ (**5**)	2.310(2)	2.37(2)		2.40(3)
$[(Tp)_2Mo_2Fe_6S_8Se(SEt)_2]^{3-}$ (**6**)	2.28(1)	2.40(2)		2.29(2)
$[(Tp)_2Mo_2Fe_6S_8Se(CN)_2]^{3-}$ (**7**)	2.321(6)	2.38(4)		1.99(1)
$\{[(Tp)_2Mo_2Fe_6S_9](\mu_2-S)\}_2^{5-}$ (**8**)	2.21(2)	2.40(4)	2.19(2)	
$\{[(Tp)_2Mo_2Fe_6S_8Se](\mu_2-Se)\}_2^{5-}$ (**9**)[e]	2.317(9)	2.41(3)	2.34(1)	

[a] Ranges of mean values: Mo−N 2.23(4)−2.5(6), Mo−S 2.36(2)−2.37(2), Fe−S 2.25(1)−2.26(2), Mo−Fe 2.70(3)−2.72(2), Fe−Fe 2.70(3)−2.76(6). [b] Within P^N-type cores. [c] Between P^N-type cores. [d] L = terminal ligand. [e] Reference 7.

Table 4. Selected Bond Angles (deg) in P^N-Type Clusters

cluster	Fe–(μ_6-S)–Fe[a]	L–Fe–(μ_6-S/Se)[b]	intra[c] Fe–(μ_2-S/Se)–Fe	inter[d] Fe–(μ_2-S/Se)–Fe[b]
$[(Tp)_2Mo_2Fe_6S_9(SH)_2]^{3-}$ (**2**)[e]	141.0(1)	104.0(1), 107.6(9)	74.69(6), 75.24(6)	
$[(Tp)_2Mo_2Fe_6S_9(CN)_2]^{3-}$ (**3**)	143.0(4)	107.1(1), 107.33(9)	75.48(8)	
$[(Tp)_2Mo_2Fe_6S_8Se(SH)_2]^{3-}$ (**4**)	140.8(1)	105.8(1), 105.99(9)	72.34(9)	
$[(Tp)_2Mo_2Fe_6S_8Se(SeH)_2]^{3-}$ (**5**)	142.8(1)	105.63(9), 106.83(8)	71.66(9)	
$[(Tp)_2Mo_2Fe_6S_8Se(SEt)_2]^{3-}$ (**6**)	146.6(2)	100.34(9), 113.8(1)	71.56(9), 73.48(8)	
$[(Tp)_2Mo_2Fe_6S_8Se(CN)_2]^{3-}$ (**7**)	145.9(3)	105.76(8), 108.91(7)	72.16(8)	
$\{[(Tp)_2Mo_2Fe_6S_9](\mu_2-S)\}_2^{5-}$ (**8**)	140.4(2)	119.1(1)−123.42(8)	74.34(8)−74.55(7)	134.74(3)
$\{[(Tp)_2Mo_2Fe_6S_8Se](\mu_2-Se)\}_2^{5-}$ (**9**)[e]	142.1(2)	119.4(1)−122.9(1)	70.62(7)−71.81(8)	130.7(1)

[a] Largest angle. [b] L = terminal ligand or μ_2-S/Se atom bridging two P^N-type cores. [c] Within P^N-type core. [d] Between P^N-type cores. [e] Reference 7.

electrospray mass spectrum of cluster **6**, presented in Figure 4, reveals the parent cluster dianion and a parent ion pair with Et_4N^+. The spectrum is similar to that of all-sulfur cluster **2**, which showed the corresponding parent ions. The *m*/*z* data and isotope distributions demonstrate the inclusion of *one* selenium atom in cluster **6**. Compounds containing **4** and **5** also afforded parent ions (cf. Experimental Section). The similarity of the ^{1}H NMR spectra of **4**−**7** ensures the same core structure for all. When cluster **1** is reacted with up to 10 equiv of SeH^-, the only product formed is **5**. In contrast, excess SH^- with **1** affords the single cubane $[(Tp)MoFe_3S_4(SH)_3]^{2-}$ in high yield.

In another experiment bearing on selenium incorporation, a solution of 0.014 mmol of **2** and 3.9 equiv of $(Et_4N)(SeH)$ in 5 mL of CD_3CN was stirred for 24 h at ambient temperature. The ^{1}H NMR spectrum revealed the presence of only **2**; no evidence of the formation of selenium-containing cluster **5** was found. Consequently, selenium incorporation does not take place by Se/S exchange involving an all-sulfur P^N-type cluster.

With one selenium atom incorporated, it must lie in a mirror plane containing the μ_6-S and two μ_2-S/Se atoms in order to be consistent with the ^{1}H NMR spectra (Figures 2 and 3). This situation is demonstrated from the X-ray structures of **4**−**7**,

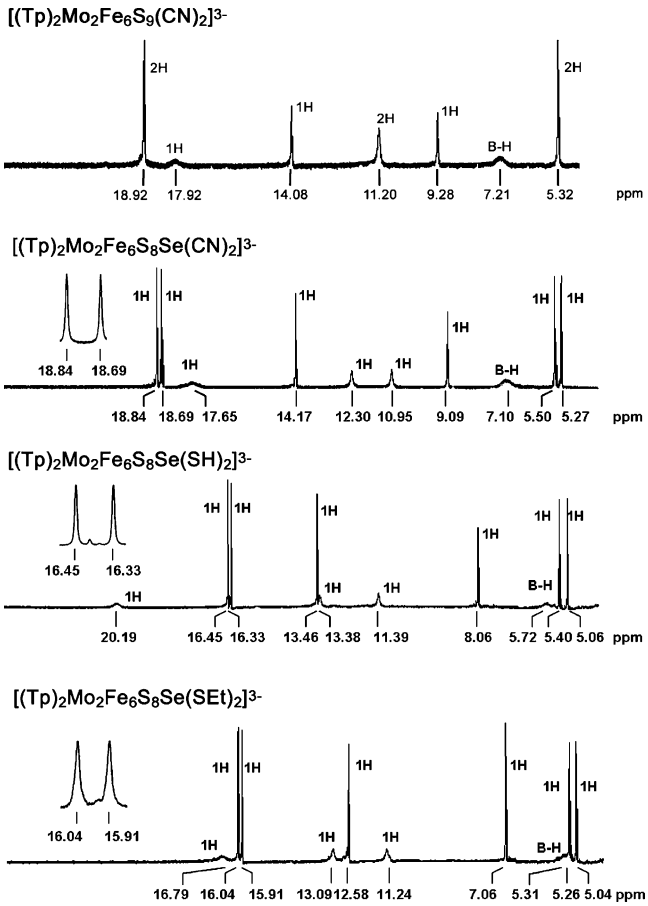

Figure 3. ^{1}H NMR spectra of P^N-type clusters $[(Tp)_2Mo_2Fe_6S_9(CN)_2]^{3-}$ (**3**), $[(Tp)_2Mo_2Fe_6S_8Se(CN)_2]^{3-}$ (**7**), $[(Tp)_2Mo_2Fe_6S_8Se(SH)_2]^{3-}$ (**4**), and $[(Tp)_2Mo_2Fe_6S_8Se(SEt)_2]^{3-}$ (**6**) in CD_3CN solutions at ambient temperature. Relative signal intensities are indicated. The insets in the range ~16−19 ppm emphasize the occurrence of two closely spaced signals in each spectrum.

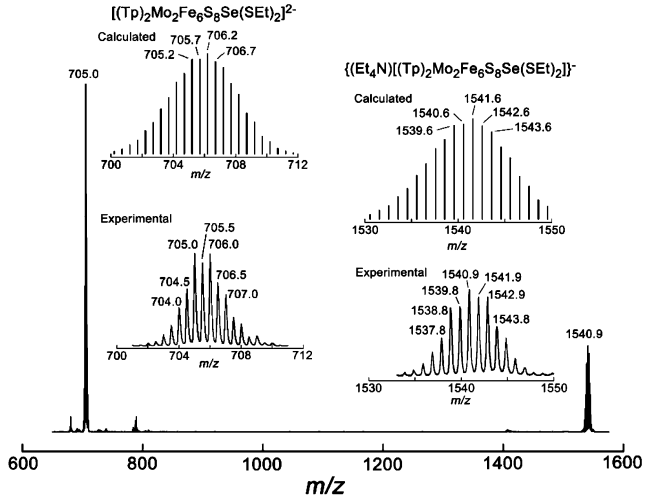

Figure 4. Electrospray negative ion experimental and calculated mass spectra of $[(Tp)_2Mo_2Fe_6S_8Se(SEt)_3]^{2-}$ (left) and an ion pair of this species and Et_4N^+ (right). Selected *m*/*z* values in the parent ion region are indicated.

which are essentially isostructural with obtuse exterior Fe−(μ_6-S)−Fe angles of 140.8(1)−146.6(2)° and acute interior Fe−(μ_2-S/Se)−Fe angles of 71.56(9)−73.48(8)°. The structures of **6** and **7** are given in Figure 5. All structures were refined with varying S/Se atom populations at all bridging positions. No evidence of Se atoms at the μ_3-sites or the unique μ_6-site was

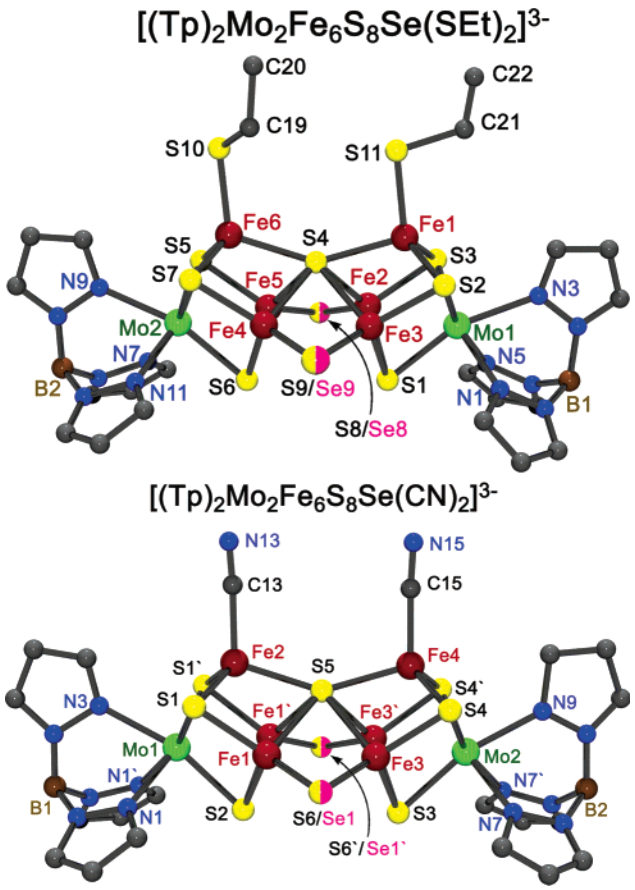

Figure 5. Structures of $[(Tp)_2Mo_2Fe_6S_8Se(SEt)_2]^{3-}$ (**6**) and $[(Tp)_2Mo_2Fe_6S_8SeOR(CN)_2]^{3-}$ (**7**). Primed and unprimed atoms are related by a crystallographic mirror plane. The apparent Se/S atom ratios are 52:48 (S8/Se8) and 57:43 (S9/Se9) in **6**, and 40:60 (S6/Se1) in **7**.

found. The most satisfactory refinements place disordered S and Se atoms at the μ_2-sites with ca. 0.5 populations. The S/Se atom ratios derived from the refinements are given in Table 1. The Fe−(μ_2-S/Se) mean bond lengths in **4**−**7** are 2.28(1)−2.321(2) Å (Table 3). These values are 0.05−0.10 Å longer than the mean Fe−(μ_2-S) distances in **2** and **3**, and thus are consistent with partial Se atom occupation at these bridging sites. Bond lengths to the μ_6-S and μ_3-S sites are not systematically affected by selenide substitution.[16] In one comparison involving the pair $[Fe_2S_2(SC_6H_4\text{-}p\text{-}Me)_4]^{2-}$/$[Fe_2Se_2(SPh)_4]^{2-}$, with bond angles (74−75°) comparable to those in the present group of clusters, the mean Fe−(μ_2-Se) bond length exceeds the Fe−(μ_2-S) value by 0.13 Å.[17,18]

Bridged P^N-Type Clusters. When cluster **2** is heated under anaerobic conditions in acetonitrile at 65 °C, the single cubane $[(Tp)MoFe_3S_4(SH)_3]^{2-}$ is formed as the principal product. Cluster **8** is also obtained in modest yield by the apparent reaction 5. The structure, shown in Figure 6, is that of a double

$$2[(Tp)_2Mo_2Fe_6S_9(SH)_2]^{3-} \rightarrow \{[(Tp)_2Mo_2Fe_6S_9](\mu_2\text{-}S)\}_2^{5-} + 2H_2S + e^- \quad (5)$$

P^N-type cluster bridged by two μ_2-S atoms. Selected metric information is contained in Tables 3 and 4. The individual clusters have different oxidation levels ($[Mo_2Fe_6S_9]^{+,2+}$) which, being related by a crystallographically imposed C_2 axis bisecting the S10−S10′ vector, are not distinguishable in the X-ray

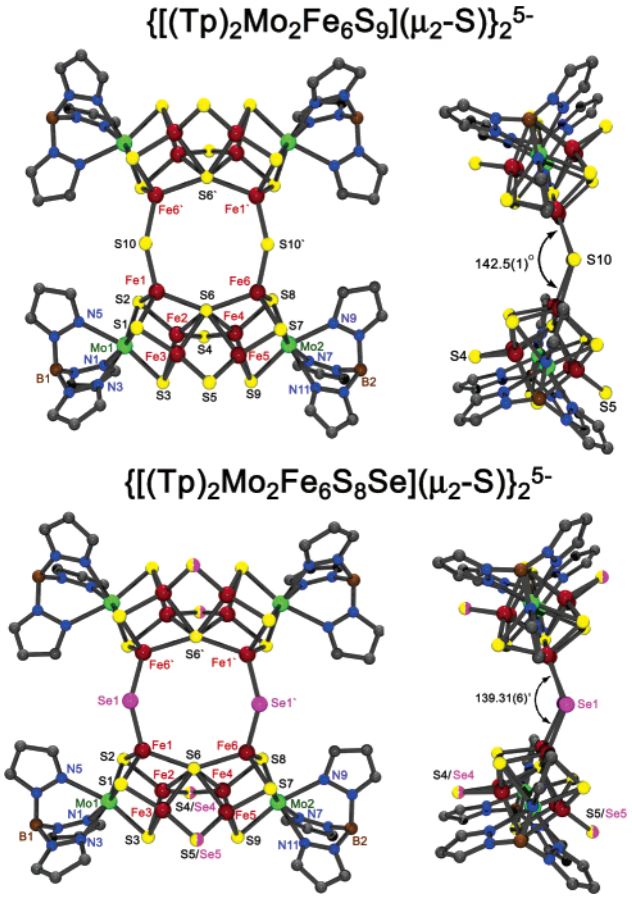

Figure 6. Structures of $\{[(Tp)_2Mo_2Fe_6S_9](\mu_2\text{-}S)\}_2^{5-}$ (**8**, upper) and $\{[(Tp)_2Mo_2Fe_6S_8Se](\mu_2\text{-}Se)\}_2^{5-}$ (**9**, lower) viewed from the front (left) and side (right). Primed and unprimed atoms are related by a crystallographic two-fold axis. Dihedral fold angles along the S10−S10′ and Se1−Se1′ vectors are specified.

structure. Evidently, the one-electron reduced form is too unstable to be isolated, similar to the products of reactions 1 and 3. Prominent in the structure is the central eight-member $Fe_4(\mu_2\text{-}S)_2(\mu_6\text{-}S)_2$ ring with internal angles in the 119−140° range. The ring is nonplanar: its two halves are folded along the S10−S10′ vector at a dihedral angle of 142.5(1)°.

A selenide-containing bridged cluster is formed more readily. In a reaction analogous to 5, an acetonitrile solution of **5**, when stirred for 4 h at ambient temperature followed by standard workup, provides the Et_4N^+ salt of **9** in 92% yield. (Note that $(Et_4N)_3$[**5**] can only be isolated only when the crystallization is performed at −35 °C.) The mass spectrum of this compound did not reveal a parent ion but displayed the species $\{[(Tp)_2Mo_2Fe_6S_8Se_3H_2]^{3-} + 4Et_4N^+\}^+$. The cell parameters of this compound are identical with those of a previously reported cluster salt prepared from the reaction of **1** and three equivalents of $(Et_4N)(SeH)$ in acetonitrile.[7] The cluster, with two μ_2-Se atoms connecting the two P^N-type units, is essentially isostructural with **8**. Chemical analysis and structure refinement suggested that both μ_2-sites within each unit were populated with Se atoms and all other bridging positions were occupied by sulfur. While we are uncertain as to the source of higher Se content by analysis in this earlier preparation, we now interpret the structure of **9** as possessing the same distribution of S/Se atoms as in **3**−**7**. The structure of **9** is depicted accordingly (Scheme 2, Figure 6).

Summary. As demonstrated by this investigation and other results from this laboratory,[7,8,13,14] EBDC clusters are highly effective precursors for the synthesis of molecules with the P^N cluster topology by the process of core conversion. While among weak-field clusters this reaction type is not common or recognized as such, a number of core conversions have been documented in iron−sulfur cluster chemistry.[31] In no case has a detailed reaction pathway been elucidated. Given the close similarities between sulfide and selenide clusters noted above, we consider selenide as a credible tracking atom for sulfide. Accordingly, we conclude that, in reaction 1, the *probable* structural fate of the attacking sulfide nucleophile is as a μ_2-S bridging atom in the P^N-type topology, and that the μ_3-S and μ_6-S atoms derive from the original content of cluster **1**. We are cognizant of the possibility that the geometry of the core structure minus the μ_6-S atom, with its 6 Mo−S + 16 Fe−S bonds, is such as to disfavor occupancy by the larger selenide atom. In this connection, we note that the μ_6-S site is subject to some structural pliability, one measure being the $\gtrsim$7° variation in the Fe−(μ_6-S)−Fe exterior angle over all known P^N-type structures (Table 4; 138.9−146.2°)[11,14,32,33] and its attendant effect on bond distances. Within a given structure, individual Fe−(μ_6-S) separations can vary by ca. 0.1 Å.[34]

The conclusion proffered is not informative as to the point of attack of sulfide or other fine details of the transformation shown in Scheme 1. However, we summarize several observations bearing on the course of the reaction. (i) Selenium inclusion does not proceed via a fully formed P^N-type cluster. (ii) Selenium occupation at μ_3-positions in the P^N-type product is ruled out by crystallographic assessment of **4**−**7**, indicating that there is little if any S/Se exchange within the reacting EDBC. (iii) Selenium incorporation is site-specific rather than being distributed over more than one site. Observations (ii) and (iii) imply that cluster fragmentation during reaction, a possibility noted at the outset, is unlikely. We do not broach any bond-making/breaking scheme for this process, for none of those considered is singularly preferable. Instead, we note the potential value of the information gained, viz., that nucleophilic attack introduces a μ_2-S element into the core structure. This raises the issue, currently under examination, as to whether other nucleophiles can be introduced as bridging atoms into the core as means of approaching the iron−molybdenum cofactor structure with its three μ_2-S and μ_6-X components.

Acknowledgment. This research was supported by NIH Grant GM 28856. We thank Dr. Richard J. Staples for useful discussions on crystallographic aspects and Matthew J. Woodcock for assistance in obtaining electrospray mass spectra.

Supporting Information Available: X-ray crystallographic information for the six compounds in Table 1 (CIF), a table of mean values of bond distances in P^N-type clusters, and experimental and calculated electrospray mass spectra in the parent ion region. This material is available free of charge via the Internet at http://pubs.acs.org.

JA063604X

(31) Rao, P. V.; Holm, R. H. *Chem. Rev.* **2004**, *104*, 527−559.
(32) Osterloh, F.; Sanakis, Y.; Staples, R. J.; Münck, E.; Holm, R. H. *Angew. Chem., Int. Ed.* **1999**, *38*, 2066−2070.
(33) Osterloh, F.; Achim, C.; Holm, R. H. *Inorg. Chem.* **2001**, *40*, 224−232.
(34) The reciprocal experiment based on the reaction of $[(Tp)_2Mo_2Fe_6Se_8(PEt_3)_4]$ and SH^- would be of interest to learn if sulfide would occupy the more capacious μ_6-Se site of the product P^N-type cluster. However, we have been unable to prepare $[(Tp)MoSe(Se_4)]^{2-}$ or another selenide-containing precursor for use in a reaction sequence[6,7] that would afford the desired EBDC.